

Damage Detection from Landsat-7 Satellite Images for the 2001 Gujarat, India Earthquake

Yalkun YUSUF¹⁾, Masashi MATSUOKA¹⁾, Fumio YAMAZAKI^{1), 2)}

1) Earthquake Disaster Mitigation Research Center
National Research Institute for Earth Science and Disaster Prevention (NIED)
2465-1Mikiyama, Miki, Hyogo 673-0433, Japan.
Tel: +81-794-83-6632, Fax: +81-794-83-6695
Email: yalkun@edm.bosai.go.jp¹⁾

2) School of Advanced Technologies
Asian Institute of Technology
P.O.Box.4, Klong Luang, Pathumthani 12120, Thailand

KEY WORDS: Optical satellite images, Landsat-7, Damage detection, the 2001 Gujarat earthquake

ABSTRACT: In this paper, we present a method of earthquake damage detection by comparing the optical images with panchromatic bands for the Gujarat, India earthquake, which occurred on January 26, 2001. The data used in this study are optical remote sensing images taken by Landsat-7 satellite on January 8 and February 29, 2001, before and after the earthquake. We investigated the pre- and post-event satellite images through calculating the differences in the reflection intensity (digital number) of the two images. The estimated impacted area was abstracted on a pixel unit based on the obtained frequency distributions of the differences in the optical sensor values, which showed significant changes in the reflectance due to the earthquake disaster. We investigated the accuracy of our analysis result using a classification method for the training areas with aerial photographs taken after the earthquake. The two damage detection methods show a very similar result.

1. INTRODUCTION

At an early stage of a large earthquake, satellite remote sensing can be a very useful method to determine damage distribution since remote sensing images cover large areas yielding detailed information of the earth's surface. There are many examples of the successful grasp of damage situations and identification of the damage areas using remote sensing images obtained from the space such as those in the case of the 1995 Kobe, Japan and the 1999 Kocaeli, Turkey earthquakes (Matsuoka et al., 2001; Estrada et al., 2000). There are also some research studies that have been conducted such as utilizing military weather satellite DMSP of U.S., using nighttime lights of cities to estimate the damaged areas (Kohiyama et al., 2000). Therefore, we can say remote sensing technology is very effective for early grasping of damage situation.

In this study, remote sensing satellite images are used to identify the areas affected by the Gujarat, India earthquake on January 26, 2001. The data used for this study are the Landsat-7 satellite images taken before and after the Gujarat earthquake. The pre-event image was acquired on January 8, 2001 and the post-event image was acquired on February 29, 2001. We investigated the pre- and post-event satellite images by calculating the differences of digital numbers of the two images. The estimated damaged area was extracted on a pixel unit based on the obtained frequency distributions of the differences in the optical sensor values, which showed significant changes in the reflectance due to the earthquake. We investigated the accuracy of our analysis result using a classification technique for the training data with the aerial photographs taken after this earthquake (IITB & EDM, 2001). The threshold values for the reflectance of the damage to the image were defined based on the values of the selected training data. Then the damage area was classified and extracted by applying the training data as a filter for the entire satellite image. A comparison was made for the results obtained by using the both damage detection methods.

2. SATELLITE IMAGE

The Landsat-7 satellite was launched on April 15 1999. The altitude of Landsat-7 is approximately 705 km with a

recurrence period of 16 days. The earth observing instrument on Landsat-7, the Enhanced Thematic Mapper Plus (ETM+), replicates the capabilities of the highly successful Thematic Mapper instruments on Landsat 4 and 5. ETM+ is an advanced, multi-spectral scanning, earth resources sensor designed to achieve higher image resolution, sharper spectral separation, more improved geometric fidelity and greater radiometric accuracy and resolution. ETM+ data are detected in eight spectral bands simultaneously. Band 6 detects thermal (heat) infrared radiation. ETM+ scene has a spatial resolution of 30 meters for bands 1-5 and 7 while band 6 has a 60-meter spatial resolution and a panchromatic band has a 15-meter spatial resolution (NASDA, 2001).

Figure 1 shows typical reflectance curves for three basic types of earth features: green vegetation, dry bare soil and water. The lines in this figure represent the average reflectance curves compiled by measuring a large sample of features, which reveal some fundamental points concerning spectral reflectance. The panchromatic images were used in this study.

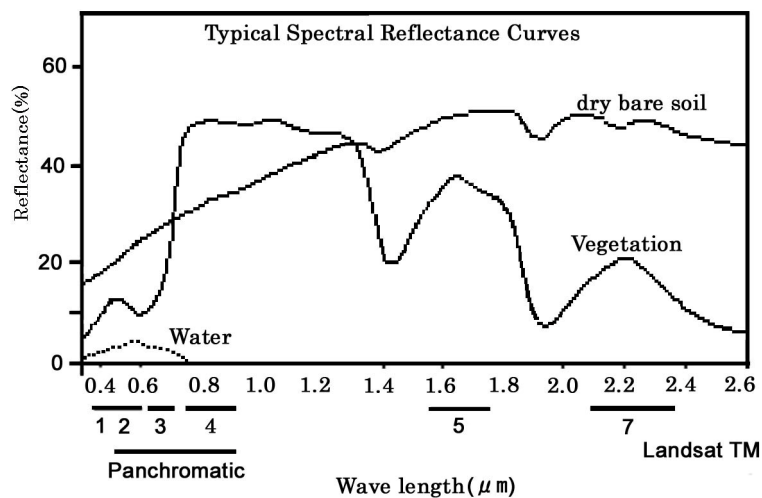
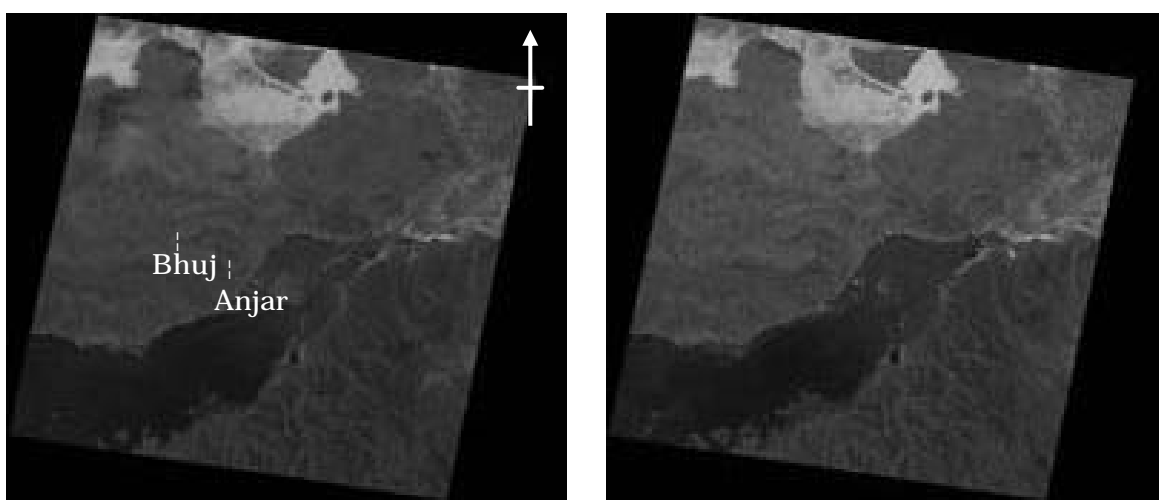


Figure 1: Typical reflectance curves for vegetation, soil and water

Figure 2 shows the pre- and post-event images of the Gujarat earthquake. Clouds did not significantly influence the two images. The two acquisition times were close together, therefore the influence of the seasons is disregarded. Image registration was carried out as a pre-processing procedure.



(a) 2001/1/8 3

(b) 2001/2/9

Figure 2: Landsat-7 panchromatic images of pre- and post-earthquake.

Figure 3 shows the target area cut from the pre- and post-earthquake panchromatic images. Figure 4 shows the

histogram of the digital numbers of the pre- and post-earthquake images. We can see that the pixel value in the post-event image is much higher than that in the pre-event image. Furthermore, comparing these images with the aerial photograph (Figure 5) taken 16 days after the earthquake, we find that brighter areas appearing in the post-event image represent the locations with severe damage. In the visible to near-infrared images, severe building damages in the urban areas show higher brightness due to brick, soil and stone from the collapsed buildings.

In this study, for damage estimation based on the classification without training data, the entire Lansat-7 satellite image was selected as the target area. For the method using training data, the Anjar region was selected as the target area, which was suffered from severe damage due to the earthquake.

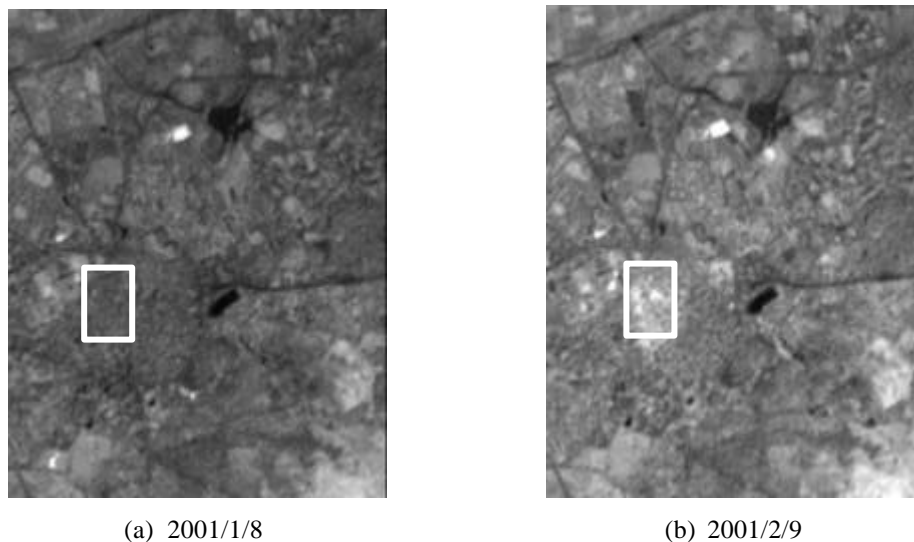


Figure 3: Pre- and post-event images of Anjar area.

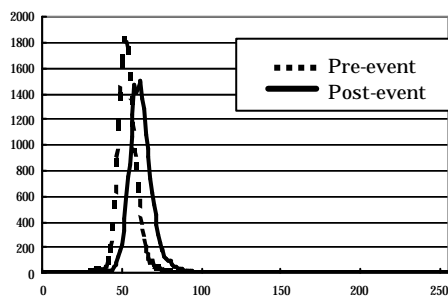


Figure 4: Histogram of pre- and post-event images. **Figure 5:** Aerial photograph taken after the earthquake.

3. DAMAGE DETECTION WITHOUT TRAINING DATA

The classification of damage areas without training data was developed based on the following principles. We investigated the pre- and post-event satellite images by calculating the differences in the reflection intensities of the both images. The impact area was extracted on a pixel unit based on the obtained frequency distributions of the differences in the optical sensor values, which showed significant changes in the reflectance due to the destruction caused by the earthquake. Compared with the pre-event image, pixels whose digital number has significantly changed in the post-event image are considered to represent damaged areas. Figure 6 shows the determination procedure for damaged areas.

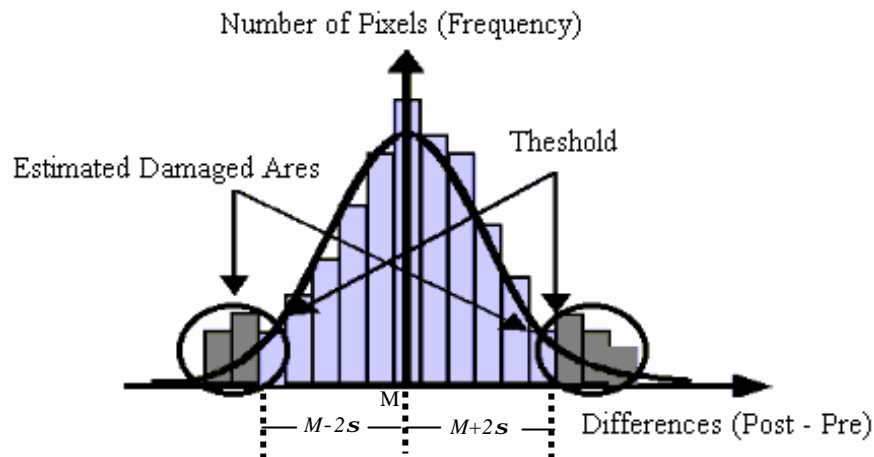
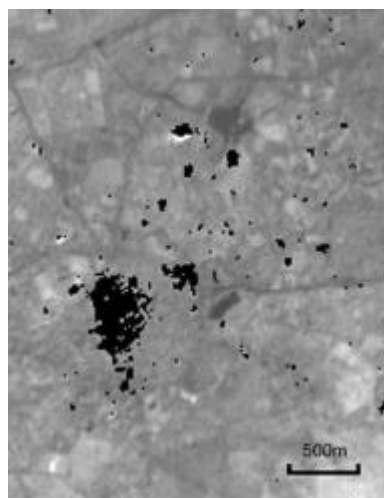


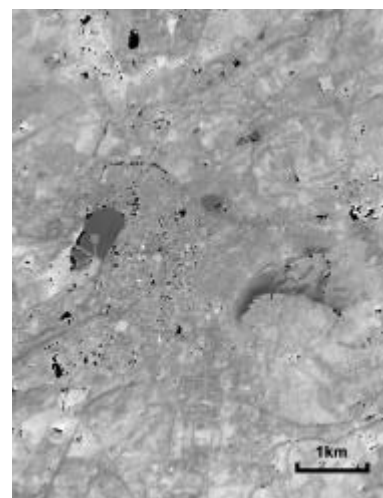
Figure 6: The determination procedure for damaged areas.

The process of damage abstraction is described as follows. First, we calculate the difference in the brightness value of post- and pre-event images. The difference can be represented as a normal distribution. Then we calculate the mean (M) and the standard deviation (S) of the difference. If the difference is over $M+2S$, the reflectance of the area is considered to be significantly increased, and if the difference value is less than $M-2S$, the reflectance of the area is considered to be significantly decreased. Both of these areas with significant changes are considered as damaged areas. We applied this method to the entire image to abstract the damaged areas.

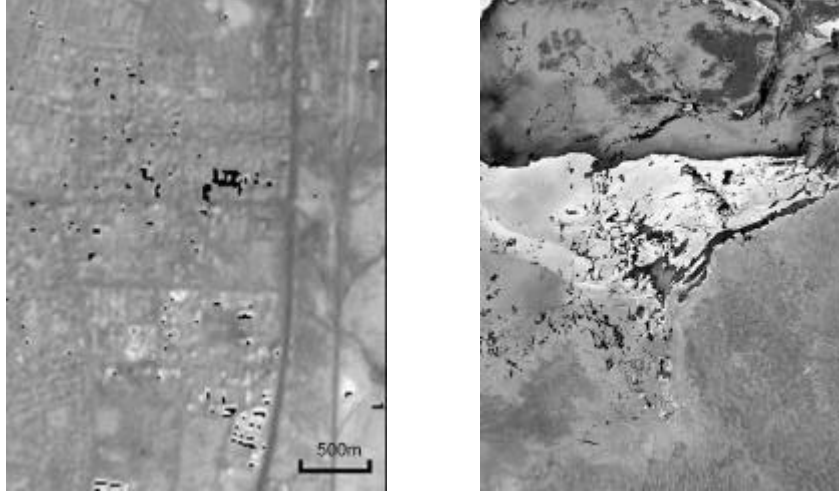
Figures 7 (a), (b), and (c) show the results of the damaged areas in Anjar, Bhuj, Gandhidam, which are zoomed in from the entire resultant images. The black pixels show the extracted damage areas. Numerous pixels were extracted in these areas using the threshold value of $M+2S$. On the other hand, a few pixels were extracted from these areas using the threshold value of $M-2S$. Comparing with the aerial photographs and field survey data, the obtained damaged areas almost corresponded with the actual damage distribution. However, numerous pixels with reduced brightness were extracted around the Banni plain, located in the north of the Kachchh area (Figure 7(d)). In this area, during the rainy season, the ground is filled up with water, and during the dry season, the water level drops and the salt in the water spreads on the surface of the earth. Both before and after the earthquake, it was the dry season in this area, thus very high brightness seen in the pre-earthquake satellite image is due to the influence of salt. However, after the earthquake, muddy ground water gushed to the surface due to liquefaction (the University of Memphis, 2001; IIT, 2001), thus the brightness level of pixels appeared to be lower in the post-earthquake satellite image.



(a) Anjar



(b) Bhuj



(c) Gandhidam

(d) Banni plain

Figure 7: Extracted damaged areas (Black pixels).

4. DAMAGE DETECTION WITH TRAINING DATA

To investigate the accuracy of the non- training data classification method result, we present a method here for estimating the damaged area, using a simple classification technique for training areas with the aerial photographs taken after this earthquake. Concerning the method of classification using a digital image of training data, many methods exist such as the maximum likelihood classifier and the minimum-distance-to-mean classifier. To realize high accuracy using these classification methods, numerous sample elements and ground-truth data are required. In this study, we applied a simple classification method. We suppose that the pixel values have a normal distribution. First, using aerial photographs, we chose training data from the original images as class C . Then, the classification was performed according to equation (1):

$$M - 2s \leq P \leq M + 2s \quad (1)$$

where M and s are the mean and the standard deviation of extracted training data, respectively, and P is the pixel digital number to be classified. If the pixel's value satisfies the equation (1), then this pixel is classified to the class C . Based on the above classification method, the damage extraction for urban areas follows four basic steps as follows:

(1) Preparation of training data

Select an urban area that was suffered from serious damage as seen in the aerial photograph as the training area (The rectangle area in Figure 3)

(2) Abstraction of urban areas

Calculate the mean and standard deviation of pixels value of the training area using the pre- earthquake image. Then classify the pixels using equation (1) to the abstracted urban area. Figure 8 (a) shows the abstracted urban area.

(3) Abstraction of damaged areas

For the extraction of damaged areas, instead of using a pre-earthquake image, use only a post-earthquake image. Figure 8 (b) shows the abstracted damaged areas, which include suburban damage areas.

(4) Abstraction of damaged urban areas

Integrating the images obtained in steps (2) and (3), damaged urban areas are extracted (Figure 8 (c)).

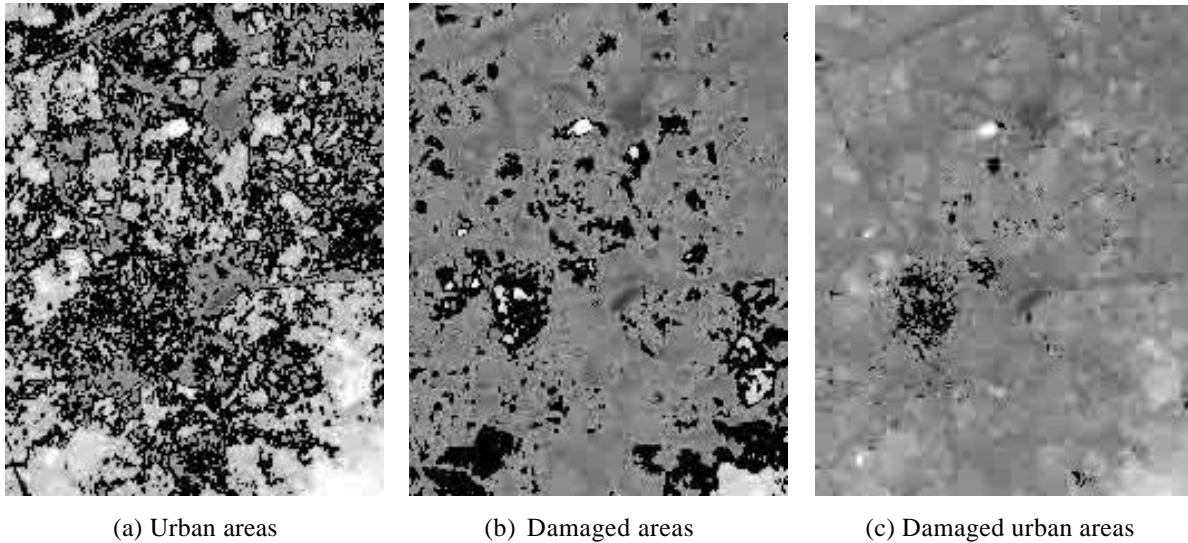


Figure 8: Classification based on the training data (Black Pixels).

5. CONCLUSION

For the purpose of grasping damage at an early stage of a large earthquake using satellite images, we present a method of earthquake damage detection by comparing the optical images with panchromatic bands of Landsat-7 satellite. The impacted areas due to the 2000 Gujarat, India earthquake are extracted by calculating the difference of the brightness values in the post- and pre-earthquake images, without using training data. As this method is applied to entire satellite images, good correspondences were shown in the most of damaged distributions that resemble the estimated results using the classification method with training data, and those identified from the post-earthquake aerial photographs. Considering the use in an emergency response immediately after an earthquake, it is difficult to obtain detailed information that can be used as training data. From a practical viewpoint, the damage estimation should be accurate without using training data.

Due to the lack of detailed damage survey data to examine the accuracy of our estimation, the analysis results are still on the level of judgment whether the area is damaged or not. In the future, we will discuss on the relationship between the damage level and the value of digital numbers based on the detailed damaged results.

REFERENCE

- Matsuoka, M. Yamazaki, F. Midorikawa, S., 2000. Characteristics of satellite optical images in areas damaged by the 1995 Hyogo-ken Nanbu Earthquake, Japan Society of Civil Engineers, No.668/I-54, pp.177-185. (in Japanese)
- Estrada, M., Matsuoka, M. and Yamazaki, F., 2000. Use of Optical Satellite Images for the Recognition of Areas Damaged by Earthquakes, 6th International Conference on Seismic Zonation, pp. 103-108..
- Kohiyama, M. et al., 2000. Development of Early Damage Area Estimation (EDES) Using DMSP/OLS Nighttime Imagery, Journal of the Institute of Social Safety Science, No. 2, pp. 79-86. (in Japanese)
- Department of Civil Engineering, India Institute of Technology Bombay (IITB), Powai, Mumbai, India, Earthquake Disaster Mitigation Research Center (EDM), National Research Institute for Earth Science and Disaster Prevention (NIED), Miki, Hyogo, JAPAN, 2001. The Bhuj Earthquake of January 26.
- NASDA, 2001. <http://landsat.gsfc.nasa.gov/main/documentation.html>.
- The University of Memphis, 2001. <http://www.ceri.memphis.edu/gujarat/report/sld008.htm>, Homepage of Center for Earthquake Research and Information.
- India Institute of Technology, 2001. <http://home.iitk.ac.in/~ramesh/gujarat/gujarat.htm>.